IMEKO TC8, TC11 and TC24 Joint Conference
October 11-13, 2023, Madeira, Portugal

EXPERIMENTAL DETERMINATION OF ABSOLUTE ROUGHNESS OF CONCRETE CONDUCTS IN A WATER SUPPLY NETWORK

L. Martins, A. Ribeiro, C. Simões, A. Pais, R. Mendes

LNEC – National Laboratory for Civil Engineering, Lisbon, Portugal, lfmartins@lnec.pt

Abstract:
This paper describes the experimental determination of the absolute roughness of concrete conducts in a pressurized water supply network related to agricultural irrigation. Based on the Colebrooke-White equation and using a Monte Carlo method, the following estimates and 95 % expanded measurement uncertainties were obtained for a circular concrete conduct with an inner diameter of 1,2 m: 0,060 mm ± 0,055 mm and 0,021 mm ± 0,024 mm, for a water flow Reynolds number, comprised between $1{,}7\cdot10^5$ and $5{,}1\cdot10^5$, respectively. The output probability distribution showed a non-symmetrical shape, and the volumetric flow and pressure drop measurements were identified as the main contributions to the obtained dispersion of roughness values.

Keywords: Hydraulics; Conduct; Concrete; Roughness

3 INTRODUCTION

Water supply networks have a massive role in our society in urban and rural areas. Water is a fundamental and essential resource for the subsistence and development of all countries and regions worldwide, justifying dedicated attention by United Nations (UN-Water) since the 1970s. These networks include several hydraulic elements such as reservoirs, dams, wells, and pumping and treatment stations, and usually have a high extension. Conducts are essential to the water transportation between the mentioned hydraulic elements, from an initial stage (collection) to the final stage (customer delivery).

From a design point of view, the friction of the water against the inner wall of conduct is a crucial issue due to the need for pumping to overcome the corresponding pressure drop along the water supply network, directly impacting construction and operation costs. The friction factor of conduct is directly related to its roughness. It is considered a complex problem in fluid mechanics, usually requiring an experimental approach under restricted conditions to obtain an accurate solution.

2 THEORETICAL BACKGROUND

In the studied hydraulic context, the conduct was considered rigid and straight, with a circular cross-section with an inner diameter D, subject to a gravitational field characterized by a g acceleration. Being V the average flow velocity inside the conduct and assuming a constant flow of a Newtonian fluid (water, in this case), the head loss, h, between two cross-sections separated by a distance L, is given by

$$h = f \cdot \frac{L}{D} \cdot \frac{V^2}{2 \cdot g}, \tag{2}$$

where f is the friction factor [1]. This dimensionless quantity is the function of the conduct roughness and the Reynolds number, Re, defined as

$$Re = \frac{V \cdot D}{\nu}, \tag{3}$$

being ν the water kinematic viscosity (considered constant in the case of an isothermal flow) [1].
In this study, the absolute (equivalent) roughness, ε_s, is assumed homogenous and uniform along the conduct, expressing the dimensional irregularities of its inner surface and considering an equal sand grain diameter (in the first roughness studies in conducts, their inner surface was coated with standard sand with a known grain dimension). In this context, the quantity relative roughness is defined by the quotient between the equivalent roughness and the conduct inner diameter, ε_s/D.
The Colebrook-White equation [1] is an implicit function which allows determining (using interpolation tables, graphical diagrams, analytical or numerical approaches) the friction factor based on the relative roughness and the Reynolds number, i.e.

$$\frac{1}{\sqrt{f}} = -2 \log\left(\frac{\frac{\varepsilon_s}{D}}{I} + \frac{M}{Re \cdot \sqrt{f}}\right), \tag{4}$$

where $I = 10^{0,87}/2$ and $M = 10^{0,4}$. If the conduct friction factor is known, the Colebrook-White equation can be used to express the absolute (equivalent) roughness explicitly:

$$\varepsilon_s = D \cdot I \left(10^{-\frac{1}{2\sqrt{f}}} - \frac{M}{Re \cdot \sqrt{f}} \right). \qquad (5)$$

By introducing the concept of equivalent hydrostatic pressure [1] in expression (1), the friction factor can be obtained from

$$f = \frac{2 \cdot \Delta p \cdot D}{\rho \cdot L \cdot V^2}, \qquad (6)$$

where ρ is the water density (for a given temperature and pressure inside the conduct), and Δp is the pressure drop between two cross-sections separated by a distance of L.

In summary, the measurement approach applied in this study for the determination of the absolute (equivalent) roughness is supported by knowledge about: (i) the water´s physical properties (known density and viscosity values from the literature, using pressure and temperature measurements); (ii) the conduct's dimensional properties (inner diameter and distance between two cross-sections); (iii) the average flow velocity (obtained from the volumetric flow measurements, q_v, knowing the inner diameter of the conduct), and; (iv) the pressure drop (based on pressure simultaneous measurements in two cross-sections of the conduct).

4 EXPERIMENTAL WORK

The following sections describe the hydraulic infrastructure where the studied concrete conduct is located, the applied experimental resources and the testing procedure.

a. Hydraulic infrastructure

The studied concrete conduct is part of a hydraulic infrastructure dedicated to agricultural irrigation at Alentejo (South region of Portugal), connecting two water reservoirs at different altitudes. Water pressurization is assured by a pumping station located near the lowest reservoir. Three measurement points were defined in this conduct (as shown in Figure 1): (i) the flow measurement near the highest reservoir; (ii) the pressure measurement in two air valves (1 and 2) installed in different cross-sections of the conduct, 804 meters away from each other, without any significant hydraulic elements between them.

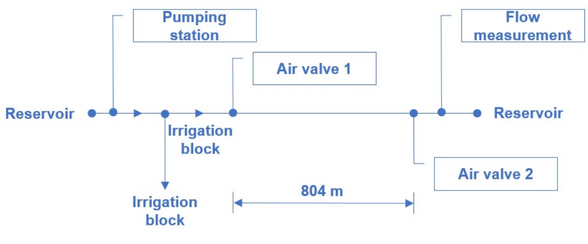

Figure 9: Schematic representation of the hydraulic infrastructure

b. Experimental resources

Table 1 mentions the measurement instruments used in the experimental work, namely, their main metrological features.

Table 1: Measurement instruments

Designation	Brand and model	Range and resolution
Pressure transducers with digital indicator	Druck; PDCR 910-1422	20 bar; 0,1 mbar
	Druck; ---	35 bar; 1 mbar
Ultrasonic flowmeter	Dynasonics; DXNP EHS-NN	1945 m^3/h; 0,01 m^3/h
Digital thermometer	Druck; DPI 605	0 ºC – 40 ºC; 0,01 ºC

These instruments are traceable to measurement standards which perform measurement units according to the International System of Units (SI) and were subjected to metrological confirmation, from which linear calibration curves were obtained for the case of the pressure measurement chains.

c. Testing procedure

Automatic data acquisition of flow, pressure and temperature measurements was defined, considering an acquisition period of five seconds during 10 minutes records.

The flowmeter was installed in the conduct considering its measurement principle (ultrasonic) and assuring the minimum recommended distance between sensors (see Figure 2), considering the conduct outer perimeter and wall thickness.

Figure 10: Flowmeter ultrasonic sensors installed in the conduct

Each pressure transducer was installed in the service plug of the air valve mounted in the conduct (see Figure 3) after water drainage and performing the measurement zero.

A water sample was collected before and after the test in one of these air valves to obtain the required temperature measurement.

Static pressure records were obtained at the beginning and end of the test without pump pressurization of the conduct. Seven volumetric flow testing steps were defined, from 550 m^3/h up to 1750 m^3/h, and the corresponding dynamic pressure measurements were performed in the two cross-sections of the conduct at the air valves.

Figure 11: Connection of the pressure transducer to one of the conduct's air valve

5 RESULTS

In the performed test, a constant water temperature was observed (20,1 ºC) between the experimental campaign's beginning and end. Based on this information and in static pressure measurements performed in each air valve (shown in Table 2), average water density (998,30 kg/m^3) and kinematic viscosity (1,0008·10^{-6} m^2/s) values were obtained from the literature [2].

Table 2: Static pressure measurement results (average values and sample experimental standard deviations)

Static pressure	Air valve 1 /bar	Air valve 2 /bar
Test beginning	5,088 3 ± 0,008 6	1,769 6 ± 0,002 1
Test end	5,088 6 ± 0,001 5	1,769 4 ± 0,001 1

Table 3 presents the average values and sample experimental standard deviations related to the flow and dynamic pressure measurements.

Table 3: Dynamic pressure measurement results for each flow testing step

Volumetric flow /m^3/h	Dynamic pressure in air valve 1 /bar	Dynamic pressure in air valve 2 /bar
576 ± 34	5,096 3 ± 0,001 0	1,772 6 ± 0,000 6
765 ± 65	5,100 1 ± 0,000 9	1,773 7 ± 0,001 1
828 ± 71	5,100 5 ± 0,000 8	1,773 4 ± 0,001 0
1020 ± 100	5,106 5 ± 0,000 7	1,775 8 ± 0,000 9
1402 ± 139	5,122 1 ± 0,001 2	1,783 5 ± 0,000 6
1676 ± 134	5,140 7 ± 0,003 8	1,794 8 ± 0,001 5
1721 ± 117	5,139 3 ± 0,003 9	1,792 9 ± 0,001 4

Based on the results shown in Tables 2 and 3, the corresponding differential pressures and pressure drops were calculated (see Table 4) and used to determine the intermediate (average flow velocity, Reynolds number and friction factor) and output (roughness) quantities. The results are shown in Table 5 and Figure 4.

Table 4: Differential pressure and pressure drop estimates

Volumetric flow /m^3/h	Differential pressure in air valve 1 /bar	Differential pressure in air valve 2 /bar	Pressure drop /bar
576	0,007 9	0,003 1	0,004 8
765	0,011 7	0,004 2	0,007 5
828	0,012 1	0,003 9	0,008 2
1020	0,018 0	0,006 3	0,011 8
1402	0,033 6	0,014 0	0,019 7
1676	0,052 2	0,025 3	0,027 0
1721	0,050 9	0,023 4	0,027 5

Table 5: Estimates for the intermediate and output quantities

Flow velocity /m/s	Reynolds number	Friction factor	Roughness /mm
0,141	1,7·10^5	0,072	0,060
0,188	2,3·10^5	0,064	0,046
0,203	2,4·10^5	0,059	0,039
0,251	3,0·10^5	0,056	0,034
0,344	4,1·10^5	0,049	0,025
0,412	4,9·10^5	0,047	0,022
0,423	5,1·10^5	0,046	0,021

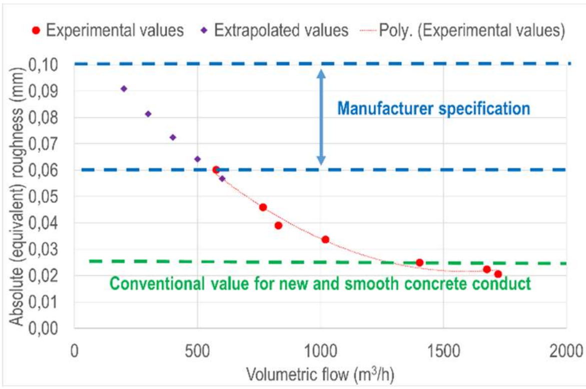

Figure 4: Relation between roughness and flow values

The determination of the measurement uncertainty related to the roughness estimates presented in Table 5 was performed using a Monte Carlo method (MCM) [3], considering the propagation of the measurement uncertainties (mentioned in Table 6) from the input quantities to the output quantity and the nonlinearity and complexity of the mathematical models involved, namely, the Colebrook-White equation. A total of 10^6 runs were performed to ensure a convergent solution for the roughness dispersion of values and a computational measurement uncertainty below 0,001 mm. The numerical simulation results are presented in Table 7.

Figure 5 shows an example of the roughness output probability distribution obtained by the MCM method, in this case, for an estimate equal to 0,023 mm.

Table 6: Probabilistic formulation of the input quantities

Uncertainty component	Type	Probability distribution	Standard uncertainty
$u(D)$	B	Gaussian	2,5 mm
$u(L)$	B	Gaussian	50 mm
$u(\rho)$	B	Gaussian	0,03 kg/m^3
$u(\nu)$	B	Gaussian	$2{,}9 \cdot 10^{-9}$ m^2/s
$u(q_v)$	A	Gaussian	34 m^3/h – 117 m^3/h
$u(p_1)$	A	Gaussian	0,7 mbar – 3,9 mbar
$u(p_2)$	A	Gaussian	0,6 mbar – 1,4 mbar

Table 7: Results of the MCM numerical simulations

Average /mm	Mode /mm	2,5 % and 97,5 % percentiles /mm	95 % expanded uncertainty /mm
0,063	0,054	0,019 ; 0,129	0,055
0,056	0,039	0,011 ; 0,123	0,056
0,043	0,033	0,011 ; 0,103	0,046
0,038	0,026	0,011 ; 0,092	0,041
0,028	0,022	0,008 ; 0,071	0,031
0,025	0,016	0,006 ; 0,063	0,028
0,023	0,017	0,006 ; 0,053	0,024

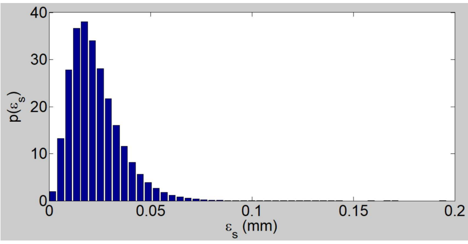

Figure 5: Example of the roughness output probability distribution

The same numerical routine was used to perform a sensitivity analysis of the input quantities to identify the main contributions to the roughness measurement uncertainty. Each input measurement uncertainty (mentioned in Table 6) was individually increased by 25 %, and the corresponding output measurement uncertainty increase was normalized. This analysis revealed that the volumetric flow quantity contributes to 53 % of the roughness uncertainty, while the pressure drop contributes to close to 44 %. The remaining input quantities have an individual contribution equal to or lower than 1 %.

6 CONCLUSIONS

The performed study allowed us to conclude that the absolute (equivalent) roughness of the concrete conduct (with a circular cross-section of 1,2 m inner diameter) is comprised between 0,060 mm and 0,021 mm, considering a water flow characterized by a Reynolds number between $1{,}7 \cdot 10^5$ and $5{,}1 \cdot 10^5$, respectively. The mentioned estimates include the additive pressure drop effect of joints and other hydraulic elements in the 804 m length conduct and of biofilm and other residues in its inner wall (expected to be reduced due to the short time of operation in agricultural irrigation).

95 % expanded measurement uncertainties varied between 0,055 mm and 0,024 mm, being related to the volumetric flow and pressure drop measurement uncertainties that are mainly originated by the hydraulic stability of the observed water flow in the conduct.

The application of the MCM allowed noticing the non-symmetrical geometrical shape of the roughness output probability distribution, which is justified by the proximity of the obtained estimates relative to the zero-roughness physical limit imposed by the Colebrook-White equation. This fact also explains the differences observed between: (i) the numerical estimates of the average and mode values shown in Table 7, and; (ii) the analytical (Table 5) and numerical (Table 7) roughness estimates.

The highest experimental roughness estimate (around 0,06 mm) is close to the expected value of the conduct's manufacturer for low volumetric flow (near 600 m^3/h). In comparison, the lowest roughness estimates are almost equal to the conventional value (0,025 mm) mentioned in the literature [4] for new and smooth concrete conduct, such as the one studied in this work.

A second-order polynomial (shown in Figure 4) can be fitted to the obtained experimental roughness and volumetric flow values, having a similar shape as the curves mentioned in hydraulic diagrams [1].

Future work will be dedicated to studying the relation between the equivalent roughness and the (non-equivalent) physical roughness directly measured in concrete conduct samples with an optical profilometer, for manufacturing quality control purposes.

7 REFERENCES

R. H. Sabersky, A. J. Acosta, E. G. Hauptmann, E. M. Gates, Fluid Flow – a first course in Fluid Mechanics. New Jersey: Prentice Hall, Ch. 5, pp. 187-202, 1999.

E. Lemmon, I. Bell, M. Huber, M. McLinden, "Thermophysical properties of fluid systems" in NIST Chemistry WebBook – NIST Standard Reference Database Number 69, 2023 Edition. Online [Accessed 20230602].

Evaluation of measurement data – Supplement 1 of the “Guide to the expression of uncertainty in measurement” – Propagation of distributions using a Monte Carlo Method. JCGM 101, Joint Committee for Guides in Metrology, 2008.

H. Ahmari, S. Kabir, Applied Fluid Mechanics Lab Manual. Mavs Open Press, 2019.